

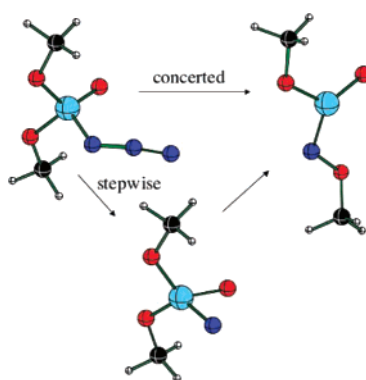
Computational Study of the Curtius-like Rearrangements of Phosphoryl, Phosphinyl, and Phosphinoyl Azides and Their Corresponding Nitrenes

Ryan D. McCulla, Gamal A. Gohar, Christopher M. Hadad,* and Matthew S. Platz*

Department of Chemistry, The Ohio State University, 100 West 18th Avenue, Columbus, Ohio 43210

hadad.1@osu.edu; platz.1@osu.edu

Received June 3, 2007



The free energies of reaction (ΔG) and activation (ΔG^\ddagger) were determined for the Curtius-like rearrangement of dimethylphosphinoyl, dimethylphosphinyl, and dimethylphosphoryl azides as well as the corresponding singlet and triplet nitrenes by CBS-QB3 and B3LYP computational methods. From CASSCF calculations, it was established that the closed-shell configuration was the lower energy singlet state for each of these nitrenes. The triplet states of dimethylphosphinyl- and dimethylphosphorylnitrene are the preferred ground states. However, the closed-shell singlet state is the ground state for dimethylphosphinoylnitrene. The CBS-QB3 ΔG^\ddagger values for the Curtius-like rearrangements of dimethylphosphinyl and dimethylphosphoryl azides were 45.4 and 47.0 kcal mol⁻¹, respectively. For the closed-shell singlet dimethylphosphinyl- and dimethylphosphorylnitrene, the CBS-QB3 ΔG^\ddagger values for the rate-limiting step of the Curtius-like rearrangement were 22.9 and 18.0 kcal mol⁻¹, respectively. It is unlikely that the nitrenes will undergo a Curtius-like rearrangement because of competing bimolecular reactions that have lower activation barriers. The pharmacology of weaponized organophosphorus compounds can be investigated using phosphorylnitrenes as photoaffinity labels. Dominant bimolecular reactivity is a desirable quality for a photoaffinity label to possess, and thus, the resistance of phosphorylnitrenes to intramolecular Curtius-like rearrangements increases their usefulness as photoaffinity labels.

Introduction

An aryl azide was first used as a photoaffinity label by Knowles and co-workers.¹ In their original experiment, they attempted to label a specific antibody. In subsequent studies involving numerous investigators, aryl azides have been used to study intramolecular interactions such as ligand–receptor and substrate–enzyme interactions.² It was generally believed that

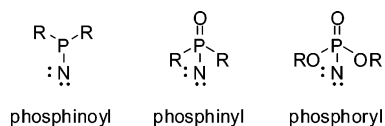
the photolysis of aryl azides produces aryl nitrenes that indiscriminately react with nearby residues and organic substrates to form robust linkages, but it was later shown that the reactive species is a ketenimine, which is more discriminate in its reactivity, and hence less desirable as a photoaffinity labeling reagent.³ We are very interested in developing indiscriminate, reactive nitrenes from photoactivatable precursors, especially ones that are suitable for photoaffinity labeling. In this vein, we considered phosphinoyl-, phosphinyl-, and phosphorylni-

(1) Knowles, J. R. *Acc. Chem. Res.* **1972**, *5*, 155–160.

(2) Meisenheimer, K. M.; Koch, T. H. *Crit. Rev. Biochem. Mol. Biol.* **1997**, *32*, 101–104.

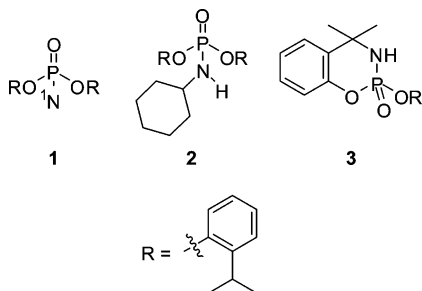
(3) Rizk, M. S.; Shi, X.; Platz, M. S. *Biochemistry* **2006**, *45*, 543–551.

trenes as possible photoaffinity agents, with each of these possible nitrenes being derived from the appropriately substituted azides.



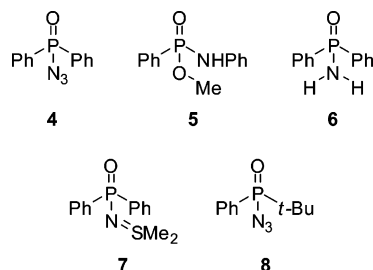
Typically, non-IUPAC nomenclature is used to describe organophosphorus compounds. The term phosphoryl- is used to abbreviate $R_2P(O)$, and phosphanyl- to describe an R_2P functional group without considering the structure of the R groups. However, IUPAC nomenclature allows for quick identification of the oxidation state of the phosphorus, which is beneficial for the discussion in this report. Therefore, we have elected to use the IUPAC nomenclature for the phosphorus compounds discussed herein.

In cyclohexane, the bis(*o*-isopropylphenoxy)phosphorylnitrene (**1**) has been found to undergo C–H bond insertion with solvent to form **2** at a rate that prevented the formation of the product **3** derived from intramolecular C–H insertion.⁴ The phosphorylnitrene **1** was also found to be less reactive toward aryl C–H bonds. Additional studies demonstrated that similar phosphorylnitrenes are less selective than acylnitrenes, which react preferentially with tertiary alkyl C–H bonds.⁵ These results suggest that phosphorylnitrenes will react within 1 ns of birth with the nearest alkyl C–H bond, which is a desirable property for a photoaffinity label.

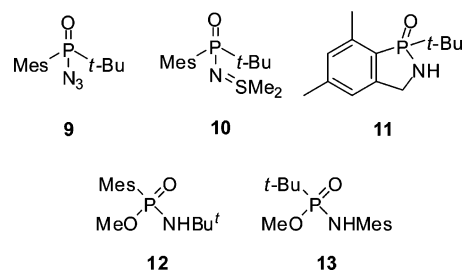


Photolysis of diphenylphosphinyl azide (**4**) extrudes N_2 , and in methanol, the final products of the reaction are the phosphonamidate (**5**) and diphenylphosphinyl amide (**6**).⁶ The phosphonamidate **5** product forms in a reaction between methanol and a Curtius-like rearrangement product of **4** that arises either in a concerted fashion with the loss of N_2 or from the singlet nitrene.⁷ In the presence of dimethyl sulfide, a known singlet nitrene trap,⁸ photolysis of **4** results in the formation of sulfilimine (**7**), the trapped nitrene product, and the amount of rearrangement product formed is reduced. However, even at the highest concentrations of dimethyl sulfide, a residual amount of rearrangement product was still observed. The authors argued that these observations indicated there was a non-nitrene (concerted) rearrangement pathway.⁸ To determine if the operat-

ing mechanism for the phosphoryl azide rearrangement was concerted, stepwise through the nitrene, or both, *t*-butylphenylphosphinic azide (**8**) was photolyzed in the presence and in the absence of dimethyl sulfide. It was observed that the ratio of phenyl and *t*-butyl rearrangement was unchanged as the concentration of dimethyl sulfide was varied. If dimethyl sulfide only suppresses the stepwise nitrene mechanism, the product ratio would remain unchanged only if the migratory aptitudes of the *t*-butyl and phenyl groups were the same for both mechanisms, which was deemed to be unlikely.



Stronger evidence for the hypothesis that the Curtius-like rearrangement occurs without traversing an intermediate nitrene was observed during the photolysis of *tert*-butyl(mesityl)phosphinic azide (**9**) in the presence of dimethyl sulfide in methanol.⁹ The photolysis of **9** resulted in two unambiguous nitrene products: the sulfilimine (**10**), derived from trapping of the nitrene by dimethyl sulfide, and the intramolecular insertion product (**11**). In addition to the nitrene products **10** and **11**, two products (**12** and **13**) arising from the Curtius-like migration of either the *tert*-butyl or mesityl group, followed by solvolysis, were also observed. Varying the concentration of dimethyl sulfide significantly increased the formation of **10** at the expense of **11**; however, the yield of **12** and **13** formed compared to that of **10** and **11** was unchanged. If the Curtius-like rearrangement was proceeding from the nitrene, increasing the concentration of dimethyl sulfide should have decreased the yield of **12** and **13** as the yield of **10** increased; however, this phenomenon was not observed.



A hallmark of superior photoaffinity labels is vigorous bimolecular reactivity, and thus, intramolecular rearrangements are inherently detrimental to the utility of a useful photoaffinity labeling reagent. We have also investigated the Curtius-like rearrangement of diazoketones, diazoesters, diazoalkanes, and sulfonylnitrenes.¹⁰ The Curtius-like rearrangement observed in phosphinyl azides, but not in phosphoryl azides, limits the potential of phosphoryl azides as photoaffinity labels. Understanding why the intramolecular Curtius-like rearrangement is prevalent for phosphinyl azides, but not for phosphoryl azides, will provide insights helpful in the design of phosphoryl azide

(4) Breslow, R.; Herman, F.; Schwabacher, A. W. *J. Am. Chem. Soc.* **1984**, *106*, 5359–5360.

(5) Breslow, R.; Feiring, A.; Herman, F. *J. Am. Chem. Soc.* **1974**, *96*, 5937–5939.

(6) Harger, M. J. P.; Westlake, S. *J. Chem. Soc., Perkin Trans. 1* **1984**, 2351–2355.

(7) Freeman, S.; Harger, M. J. P. *J. Chem. Soc., Perkin Trans. 1* **1989**, 571–578.

(8) Harger, M. P.; Westlake, S. *Tetrahedron Lett.* **1982**, *23*, 3621–3622.

(9) Harger, M. J. *J. Chem. Res.* **1993**, 334–335.

(10) Liu, J. Ph.D. Thesis, Ohio State University, Columbus, OH.

photoaffinity labels. In this report, we use computational methods to investigate if the Curtius-like rearrangement can proceed through a nitrene intermediate. This is a first step in determining the significance of these rearrangements to the application of these compounds as photoaffinity labels. Ultimately, we are interested in the entire photochemical mechanism of phosphoryl azides; however, the excited state chemistries of the azides are not discussed in this report. (We have recently reported on the rearrangements in the photochemical excited states of aryl azides.¹¹) The chemistry of a nitrene intermediate will be dominated by either the triplet state or lowest energy singlet state of the nitrene, and thus, examination of the excited state may not be required to understand the chemistry of the nitrene. In this report, we have used computational approaches to investigate the thermal Curtius-like rearrangement and the complete potential energy surfaces of dimethylphosphinoyl-, dimethylphosphinyl- and dimethylphosphoryl azides and the corresponding nitrenes.

Computational Details

Density functional theory (DFT),¹² CASSCF,¹³ and CBS-QB3¹⁴ methods have been applied in this study. To examine the excited state potential energy surface and to determine the lowest energy singlet state of the nitrenes, the multireference CASSCF/6-31G(d,p) method was employed. Multiple sizes of the active space and different optimized geometries were used for these calculations, as discussed later. The orbitals were selected to maximize the flexibility of the wave function describing the nitrene component of the molecule. The selection of these active spaces will be discussed in detail in the next section. Dimethylphosphinoyl-, dimethylphosphinyl- and dimethylphosphorylnitrene were optimized at DFT and CASSCF levels of theory. The resulting geometries from both of these methods were used in CASSCF/6-31G(d,p) calculations to examine the excited and ground state potential energy surfaces. Details of these calculations will be expanded upon in the next section. All of the CASSCF energies are presented as “bottom-of-the-well” energies, and the CASSCF calculations were performed using the GAMESS suite of programs.¹⁵ The geometries were visualized and orbitals rendered using the MacMolPlt program.¹⁶

For DFT calculations, all of the molecular geometries were optimized at the B3LYP/6-31G(d) level of theory.^{17,18} Analytical second derivatives of the energy were calculated to classify the nature of every stationary point, to determine the harmonic vibrational frequencies, and to provide zero-point vibrational energy corrections, which were scaled by a factor of 0.9806.¹⁹ The thermal and entropic contributions to the free energies were also obtained

from the B3LYP/6-31G(d) vibrational frequency calculations, using the unscaled frequencies. Using six Cartesian d functions, the energies of the B3LYP/6-31G(d) optimized structures were further refined at the B3LYP/6-311+G(d,p) level. Transition states were confirmed to connect to reactants and products either by intrinsic reaction coordinate²⁰ calculations or by careful optimization (opt = calcf) to the respective minimum after slight displacement (<10%) along the reaction path for the normal coordinate of the imaginary vibrational frequency.

More rigorous complete basis set (CBS) methods²¹ were used to increase confidence in the quantitative accuracy of the computational results. All of the stationary points were fully characterized at the CBS-QB3 level. The CBS-QB3 free energies at 298.15 K were obtained using the procedures implemented in the Gaussian03²² software package. All DFT and CBS-QB3 methods were performed using Gaussian 03 at the Ohio Supercomputer Center. Unless noted otherwise, energies are presented as CBS-QB3 free energies at 298 K.

Results and Discussion

The three possible nitrene electronic states that could possibly undergo a Curtius-like rearrangement are the open-shell singlet, closed-shell singlet, and triplet states. The chemistry of open-shell singlet and triplet nitrenes resembles that of biradicals, whereas closed-shell singlet nitrenes are more similar to electrophiles and nucleophiles, and thus, the electronic state of a nitrene has a critical influence on its expected chemistry. For the singlet states of nitrenes, either the open-shell or closed-shell configuration can be preferred depending on the structure of the nitrene.²³

Multireference Calculations. Nitrenes have two similar p orbitals to accommodate the nonbonding electrons on nitrogen. In the closed-shell singlet configuration, both electrons occupy the same p orbital, whereas in the open-shell singlet configuration, the electrons are in different p orbitals. To accurately describe the open-shell singlet nitrene, a multireference wave function is needed.¹² On the other hand, the closed-shell singlet nitrene can be described using a more computationally expedient, single-reference wave function. For accurate modeling of the expected nitrene chemistry and computational efficiency, it is important to determine the nature of the singlet nitrene as either an open-shell or closed-shell state. For dimethylphosphinoyl-, dimethylphosphinyl-, and dimethylphosphorylnitrene, this determination was made using CASSCF calculations.

Before examining the results, the selection of the active spaces employed in this study should be discussed. For ease of

(11) (a) Burdzinski, G. T.; Gustafson, T. L.; Hackett, J. C.; Hadad, C. M.; Platz, M. S. *J. Am. Chem. Soc.* **2005**, *127*, 13764–13765. (b) Burdzinski, G.; Hackett, J. C.; Wang, J.; Gustafson, T. L.; Hadad, C. M.; Platz, M. S. *J. Am. Chem. Soc.* **2006**, *128*, 13402–13411. (c) Wang, J.; Kubicki, J.; Burdzinski, G.; Hackett, J. C.; Gustafson, T. L.; Hadad, C. M.; Platz, M. S. *J. Org. Chem.* **2007**, *72*, 7581–7586.

(12) Labanowski, J. W.; Andzelm, J. *Density Functional Methods in Chemistry*; Springer: New York, 1991.

(13) Cramer, C. J. *Essentials of Computational Chemistry*, 2nd ed.; Wiley: Chichester, England, 2004; pp 487–518.

(14) Montgomery, J. A., Jr.; Frisch, M. J.; Ochterski, J. W.; Petersson, G. A. *J. Chem. Phys.* **1999**, *110*, 2822–2827.

(15) Schmidt, M. W.; Baldridge, K. K.; Boatz, J. A.; Elbert, S. T.; Gordon, M. S.; Jensen, J. H.; Koseki, S.; Matsunaga, N.; Nguyen, K. A.; Su, S.; Windus, T. L.; Dupuis, M.; Montgomery, J. A. *J. Comput. Chem.* **1993**, *14*, 1347–1363.

(16) Bode, B. M.; Gordon, M. S. *J. Mol. Graphics Model.* **1998**, *16*, 133–138.

(17) Lee, C.; Yang, W.; Parr, R. G. *Phys. Rev. B* **1988**, *37*, 785–789.

(18) Becke, A. D. *J. Chem. Phys.* **1993**, *98*, 5648–5642.

(19) Scott, A. P.; Radom, L. *J. Phys. Chem.* **1996**, *100*, 16502–16513.

(20) Fukui, K. *Acc. Res. Chem.* **1981**, *14*, 363–368.

(21) Montgomery, J. A.; Frisch, M. J.; Ochterski, J. W.; Petersson, G. A. *J. Chem. Phys.* **2000**, *112*, 6532–6542.

(22) Frisch, M. J.; Trucks, G. W.; Schlegel, H. B.; Scuseria, G. E.; Robb, M. A.; Cheeseman, J. R.; Montgomery, J. A., Jr.; Vreven, T.; Kudin, K. N.; Burant, J. C.; Millam, J. M.; Iyengar, S. S.; Tomasi, J.; Barone, V.; Mennucci, B.; Cossi, M.; Scalmani, G.; Rega, N.; Petersson, G. A.; Nakatsuji, H.; Hada, M.; Ehara, M.; Toyota, K.; Fukuda, R.; Hasegawa, J.; Ishida, M.; Nakajima, T.; Honda, Y.; Kitao, O.; Nakai, H.; Klene, M.; Li, X.; Knox, J. E.; Hratchian, H. P.; Cross, J. B.; Bakken, V.; Adamo, C.; Jaramillo, J.; Gomperts, R.; Stratmann, R. E.; Yazyev, O.; Austin, A. J.; Cammi, R.; Pomelli, C.; Ochterski, J. W.; Ayala, P. Y.; Morokuma, K.; Voth, G. A.; Salvador, P.; Dannenberg, J. J.; Zakrzewski, V. G.; Dapprich, S.; Daniels, A. D.; Strain, M. C.; Farkas, O.; Malick, D. K.; Rabuck, A. D.; Raghavachari, K.; Foresman, J. B.; Ortiz, J. V.; Cui, Q.; Baboul, A. G.; Clifford, S.; Cioslowski, J.; Stefanov, B. B.; Liu, G.; Liashenko, A.; Piskorz, P.; Komaromi, I.; Martin, R. L.; Fox, D. J.; Keith, T.; Al-Laham, M. A.; Peng, C. Y.; Nanayakkara, A.; Challacombe, M.; Gill, P. M. W.; Johnson, B.; Chen, W.; Wong, M. W.; Gonzalez, C.; Pople, J. A. *Gaussian 03*, revision C.02; Gaussian, Inc.: Wallingford, CT, 2004.

(23) Borden, W. T.; Gritsan, N. P.; Hadad, C. M.; Karney, W. L.; Kemnitz, C. R.; Platz, M. S. *Acc. Chem. Res.* **2000**, *33*, 765–771.

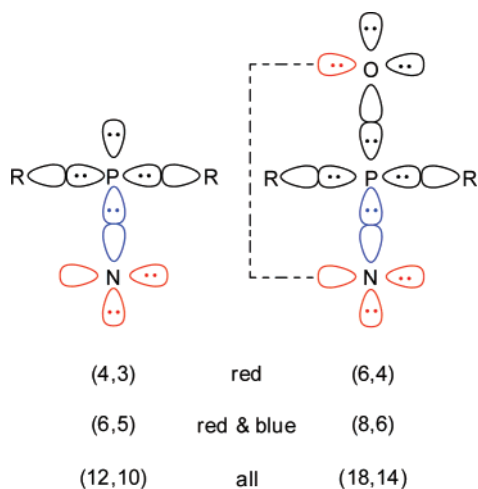


FIGURE 1. Visual diagram of the orbitals and electrons included in the CASSCF active spaces.

reference, a diagram of the valence orbitals and electrons in the different active spaces is shown in Figure 1. The diagram does not convey any geometric information, but it is a useful visual aid for the counting of orbitals and electrons included in the active spaces. In Figure 1, bonds are represented by paired orbitals, and empty or occupied nonbonding orbitals are represented by unpaired orbitals. If a bond was to be included in an active space, then the bonding and antibonding orbitals were included in the active space. The closed-shell singlet electronic configuration is shown in Figure 1. The electronic configuration of the open-shell singlet and triplet nitrene could be achieved by moving one of the nonbonding lone pair of electrons on the nitrogen into the empty orbital on nitrogen.

Since smaller active spaces require less computational resources than larger ones, there was an incentive to determine the smallest active space needed to accurately estimate the energy differences between the states. For dimethylphosphinoylnitrene, the smallest active space, which was considered, included all of the nonbonding valence orbitals on the nitrogen, namely, the two p orbitals and the sp orbital lone pair. These orbitals have a total of four electrons to be included in the three orbital active spaces to give a (4,3) active space.

For the closed-shell singlet state of dimethylphosphinyl- and dimethylphosphorylnitrene, there is overlap between the empty p orbital on nitrogen and the lone pair on oxygen, forming a weak interaction as shown in Figure 2. This weak N...O interaction and corresponding antibonding interaction were included in the active space for the phosphinyl- and phosphorylnitrene, thereby creating a (6,4) active space. This interaction is illustrated in Figure 1 by the dotted line.

An intermediate active space examined included the P–N σ bonding orbital, the corresponding s^* antibonding orbital, as well as the orbitals and electrons mentioned earlier to form a (6,5) active space for phosphinoylnitrene and a (8,6) active space for phosphinyl- and phosphorylnitrene. The inclusion of all of these bonding orbitals, antibonding orbitals, and lone pair orbitals on phosphorus, oxygen, and nitrogen formed the largest active space, which was (12,10) for dimethylphosphinoylnitrene and (18,14) for dimethylphosphinyl- and dimethylphosphorylnitrene.

To determine which configuration and state were preferred for dimethylphosphinoyl-, dimethylphosphinyl-, and dimethylphosphorylnitrene, their geometries for the closed-shell singlet

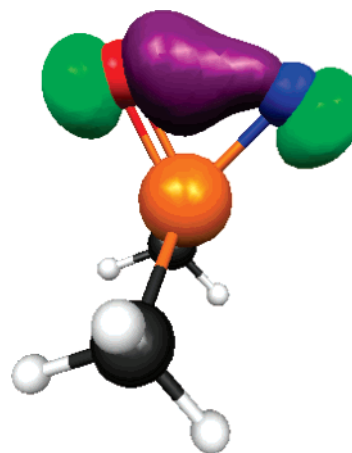


FIGURE 2. Highest occupied (natural) molecular orbital of dimethylphosphinoylnitrene at the CASSCF(6,4)/6-31G(d,p) level of theory, displaying the weak N...O interaction. The orbital was rendered using a contour value of 0.124 au.

and triplet states were initially optimized at the B3LYP/6-31G(d) levels of theory. These geometries were then used for starting geometries in CASSCF/6-31G(d,p) geometry optimizations. For dimethylphosphinoylnitrene, the CASSCF/6-31G(d,p) geometry optimization was performed for all of the previously mentioned active spaces ((4,3), (6,5), and (12,10)). For dimethylphosphinyl- and dimethylphosphorylnitrene, the CASSCF/6-31G(d,p) geometry optimizations were performed using the (6,4) and (8,6) active spaces. Geometry optimizations at the CASSCF(18,14)/6-31G(d,p) level of theory were found to be cumbersome with one optimization step requiring more than 1 day running in parallel on two processors. Thus, it was concluded that the benefit of determining the optimized geometry of the nitrenes at the CASSCF(18,14)/6-31G(d,p) level was not worth the computational expense. Unfortunately, the convergence of the open-shell singlet nitrene wave function near the optimized geometry was often unstable. Thus, to achieve convergence near the optimized geometries, the geometries of the open-shell singlet dimethylphosphinyl- and dimethylphosphorylnitrene were restricted to be C_s symmetry. For dimethylphosphinoylnitrene, the CASSCF(6,5)/6-31G(d,p) and CASSCF(12,10)/6-31G(d,p) open-shell singlet geometry optimizations converged using C_1 symmetry. The CASSCF(4,3)/6-31G(d,p) open-shell singlet wave function did not converge at any symmetry. The values for some important geometrical parameters are given in Table 1. For the closed-shell singlet, open-shell singlet, and triplet states, graphical renderings of the CASSCF(6,5)/6-31G(d,p) geometries for dimethylphosphinoylnitrene and CASSCF(8,6)/6-31G(d,p) geometries for dimethylphosphinyl- and dimethylphosphorylnitrene are shown in Figure 3.

Regardless of the active space, all of the open-shell singlet nitrenes have optimized CASSCF/6-31G(d,p) geometries that are more similar to their corresponding triplet state geometries than their closed-shell singlet state geometries. The geometric difference between the closed-shell singlet state relative to the open-shell singlet and triplet states is most apparent in the P–N bond length and the O–P–N bond angle. For most of the nitrenes, the P–N bond length for the closed-shell singlet nitrene is on average 0.15 Å shorter than the same bond of the open-shell singlet and triplet state. The only notable exception is for dimethylphosphinoylnitrene whose triplet state P–N bond length

TABLE 1. P–N, P–O, P–CH₃, P–OCH₃ Bond Lengths and the O–P–N Bond Angle for the Open-Shell and Closed-Shell Singlet and Triplet States of Dimethylphosphinoyl-, Dimethylphosphinyl-, and Dimethylphosphorylnitrene

	P–N ^a	P–R ^b	P–O ^a	O–P–N ^c
Phosphinoylnitrene Closed-Shell Singlet				
B3LYP/6-31G(d)	1.52	1.85		
CASSCF(4,3)/6-31G(d,p)	1.51	1.83		
CASSCF(6,5)/6-31G(d,p)	1.52	1.83		
CASSCF(12,10)/6-31G(d,p)	1.52	1.84		
Phosphinoylnitrene Open-Shell Singlet				
CASSCF(4,3)/6-31G(d,p)	<i>d</i>	<i>d</i>		
CASSCF(6,5)/6-31G(d,p)	1.64	1.83		
CASSCF(12,10)/6-31G(d,p)	1.63	1.84		
Phosphinoylnitrene Triplet				
B3LYP/6-31G(d)	1.70	1.87		
CASSCF(4,3)/6-31G(d,p)	1.75	1.85		
CASSCF(6,5)/6-31G(d,p)	1.79	1.85		
CASSCF(12,10)/6-31G(d,p)	1.76	1.89		
Phosphinylnitrene Closed-Shell Singlet				
B3LYP/6-31G(d)	1.62	1.82	1.57	70.1
CASSCF(6,4)/6-31G(d,p)	1.58	1.80	1.55	79.3
CASSCF(8,6)/6-31G(d,p)	1.61	1.81	1.56	70.1
Phosphinylnitrene Open-Shell Singlet				
CASSCF(6,4)/6-31G(d,p)	1.73	1.81	1.46	113.8
CASSCF(8,6)/6-31G(d,p)	1.76	1.81	1.47	113.9
Phosphinylnitrene Triplet				
B3LYP/6-31G(d)	1.75	1.83	1.50	113.1
CASSCF(6,4)/6-31G(d,p)	1.75	1.81	1.46	113.6
CASSCF(8,6)/6-31G(d,p)	1.79	1.81	1.47	113.7
Phosphorylnitrene Closed-Shell Singlet				
B3LYP/6-31G(d)	1.60	1.59	1.54	75.9
CASSCF(6,4)/6-31G(d,p)	1.56	1.56	1.53	81.5
CASSCF(8,6)/6-31G(d,p)	1.56	1.56	1.54	79.1
Phosphorylnitrene Open-Shell Singlet				
CASSCF(6,4)/6-31G(d,p)	1.71	1.57	1.45	114.1
CASSCF(8,6)/6-31G(d,p)	1.74	1.57	1.45	114.2
Phosphorylnitrene Triplet				
B3LYP/6-31G(d)	1.73	1.60	1.48	112.1
CASSCF(6,4)/6-31G(d,p)	1.73	1.57	1.45	112.2
CASSCF(8,6)/6-31G(d,p)	1.77	1.57	1.45	112.2

^a Values of the P–N and P–O bond lengths in angstroms. ^b Values of the P–CH₃ bond length for dimethylphosphinoyl- and dimethylphosphinylnitrene and the P–OCH₃ bond length for dimethylphosphorylnitrene in angstroms. ^c Values of the O–P–N bond angle in degrees for dimethylphosphinyl- and dimethylphosphorylnitrene. ^d SCF did not converge.

is roughly 0.25 Å longer than the same bond of the closed-shell singlet state.

For the dimethylphosphinyl- and dimethylphosphorylnitrenes, the O–P–N bond angle increases from approximately 75°. This is because a weak interaction forms between a lone pair orbital on oxygen and the empty p orbital on nitrogen in the closed-shell singlet state as illustrated in Figure 2. The weak N···O interaction of the closed-shell singlet of phosphinyl- and phosphorylnitrene is reminiscent of the interaction in carbonyl-substituted nitrenes.²⁴ Acylnitrenes that have singlet ground states also have O–C–N bond angles that are less than 90°. For example, the photolysis of benzoyl azide in an argon matrix at 12 K revealed that the ground state of benzoylnitrene has a structure similar to that of oxazirone. Because of the weak N···O interaction, the calculated phosphinyl- and phosphorylnitrene structures are similar to the experimentally observed structures of benzoylnitrene and other carbonyl-substituted nitrenes.

In the open-shell singlet and triplet states, the O–P–N bond angle increases from approximately 75° to approximately 113°. In the open-shell singlet or triplet state, the p orbital that was empty in the closed-shell singlet configuration is filled by a single electron. The larger O–P–N bond angle for the open-shell singlet and triplet nitrene is in response to the electron repulsion between the lone pair of oxygen and the singly filled nitrogen p orbital. The diradical characters of the open-shell singlet and triplet state are shown in Figure 4.

Nitrene Electronic State Energies. The lower energy electronic configuration of the singlet nitrene will dominate the expected chemistry of the singlet nitrene, and thus, the relative energies of the open-shell singlet, closed-shell singlet, and triplet states of the nitrenes have been determined. The energy differences for open-shell singlet and closed-shell singlet nitrenes at multiple geometries, as well as the energy differences between triplet and closed-shell singlet nitrenes are given in Table 2. For all of the active spaces employed, the preferred singlet state is the closed-shell configuration for every dimethylphosphorus-substituted nitrene that was examined, which is also the case for carbonyl-substituted nitrenes.²⁴ The triplet states of dimethylphosphinyl- and dimethylphosphorylnitrene are the ground states. However, the closed-shell singlet state is the ground state for dimethylphosphorylnitrene.

The singlet–triplet energy gap influences the rate of inter-system crossing, which is important to the expected chemistry of nitrenes. Since the closed-shell singlet is the preferred configuration for all of the examined nitrenes, the singlet–triplet energy gap is the energy difference between the closed-shell singlet and triplet state of the nitrene. Under the triplet heading in Table 2, the B3LYP, CBS-QB3, and CASSCF calculated values of the singlet–triplet gap are given where a positive number indicates a singlet ground state. The CBS-QB3 singlet–triplet energy gaps are the most reliable,²¹ and thus, they can be used to benchmark the other methods.

For dimethylphosphorylnitrene, the closed-shell singlet state is the ground state. The CASSCF(12,10)/6-31G(d,p) singlet–triplet gap is 28.7 kcal mol^{−1}, which is in fair agreement with the benchmark CBS-QB3 singlet–triplet gap of 24.4 kcal mol^{−1}. The phosphinoylnitrene closed-shell singlet electronic configuration is stabilized by the formation of a π bond between the phosphorus lone pair and the empty p orbital on the nitrogen. This π bond is shown in Figure 5. The inclusion of the π bond in the (12,10) active space of the phosphinoylnitrene is necessary to calculate energies similar to the CBS-QB3 results. When the phosphinoyl π bond is left out of the active space, as in the (4,3) and (6,5) cases, the energy of the closed-shell singlet is underestimated ~20 kcal mol^{−1}, which results in a significant underestimation of the singlet–triplet energy.

The CBS-QB3 singlet–triplet energy gaps are −15.7 and −13.8 kcal mol^{−1} for dimethylphosphinyl- and dimethylphosphorylnitrene, respectively. The predicted singlet–triplet energy gaps of the most inclusive CASSCF(18,14) active spaces are −30.7 and −22.8 kcal mol^{−1} for dimethylphosphinyl- and dimethylphosphorylnitrene, respectively. The triplet state of the phosphorylnitrenes is the ground state because, unlike phosphinoylnitrene, the phosphorus–oxygen bond precludes the formation of the phosphorus–nitrogen π bond. Without the π bond stabilization of the closed-shell nitrene, the triplet state of the nitrene becomes the lower energy state. Also, the singlet–triplet energy gaps determined with the smaller (8,6) and (6,4) active spaces for dimethylphosphinyl- and dimethylphospho-

(24) Pritchina, E. A.; Gritsan, N. P.; Bally, T. *Russ. Chem. Bull. Int. Ed.* **2005**, *54*, 525–532.

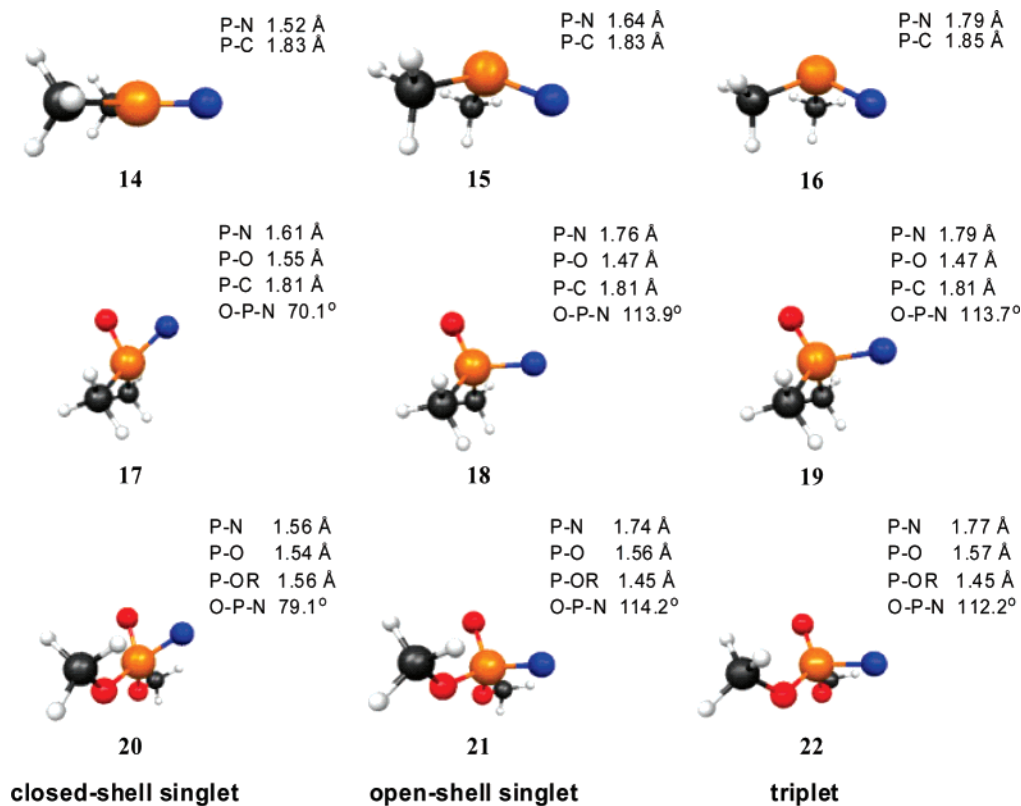


FIGURE 3. Graphical renderings of the closed-shell singlet, open-shell singlet, and triplet states at their CASSCF(6,5)/6-31G(d,p) geometries for dimethylphosphinoylnitrene (12–14) and CASSCF(8,6)/6-31G(d,p) geometries for dimethylphosphinylnitrene (15–17) and dimethylphosphorylnitrene (18–20).

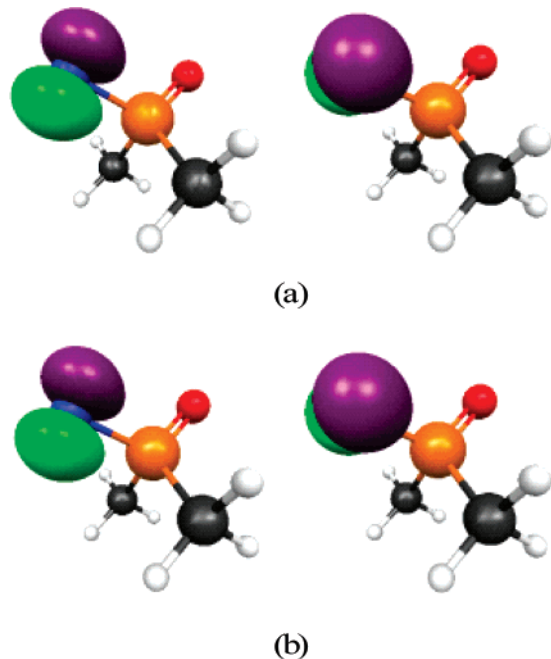


FIGURE 4. Singly occupied (natural) molecular orbitals of (a) triplet and (b) open-shell singlet states of dimethylphosphinylnitrene at the CASSCF(6,4)/6-31G(d,p) level of theory. The orbital was rendered using a contour value of 0.108 au.

rylnitrene are within 5 kcal mol⁻¹ of the (18,14) values. The consistent performance of CASSCF methods with different active spaces indicates that the inclusion of the σ bonds and

lone pairs is not critical as long as the active space includes the weak N \cdots O interaction.

The most important result obtained with the CASSCF calculations was the finding that the closed-shell singlet state was the preferred configuration for all of the examined nitrenes. Since the open-shell singlet nitrene has to be represented by a multireference wave function, CASSCF calculations were required because CBS-QB3 methods cannot treat open-shell singlet states. The CASSCF calculations confirmed that the closed-shell singlet was preferred over the open-shell singlet state for these nitrenes. Thus, the closed-shell singlet configuration will dominate the singlet nitrene chemistry, and since the closed-shell nitrene can be accurately modeled with a single-reference wave function, the more rigorous single-reference CBS-QB3 method can be used to model the Curtius-like rearrangements of the singlet nitrenes.

The failure of the CASSCF methods to replicate the CBS-QB3 singlet–triplet energy gaps was not due to an insufficient active space. The preceding results indicate that the size of the active space was less important than including the P–N π bond for phosphinoylnitrenes and the weak N \cdots O interaction for phosphinyl- and phosphorylnitrenes in the active space. Including dynamic electron correlation, by using methods such as CAS-MP2 or CASPT2,²⁵ may be required for the quantitative prediction of energy differences for these nitrenes. However, these calculations were not pursued because the qualitative CASSCF results were sufficient to establish the closed-shell singlet as the lowest energy singlet state.

(25) Serrano-Andrés, L.; Merchán, M. *J. Mol. Struct.: THEOCHEM* **2005**, *729*, 99–108.

TABLE 2. Energy Differences (kcal mol⁻¹) for the Open-Shell Singlet and Triplet Nitrenes Compared to Those of the Closed-Shell Singlet Nitrene for Dimethylphosphinoyl-, Dimethylphosphinyl-, and Dimethylphosphorylnitrene^a

	phosphinoyl-	phosphinyl-	phosphoryl-
Open-Shell Singlet at Closed-Shell Geometry ^b			
CASSCF(4,3)/6-31G(d,p)	63.2		
CASSCF(6,4)/6-31G(d,p)		44.5	44.0
CASSCF(6,5)/6-31G(d,p)	75.6		
CASSCF(8,6)/6-31G(d,p)		53.6	49.8
CASSCF(12,10)/6-31G(d,p)	90.9		
CASSCF(4,3)/6-31G(d,p)// B3LYP/6-31G(d)	71.4		
CASSCF(6,4)/6-31G(d,p)// B3LYP/6-31G(d)		61.0	52.9
CASSCF(6,5)/6-31G(d,p)// B3LYP/6-31G(d)	76.5		
CASSCF(8,6)/6-31G(d,p)// B3LYP/6-31G(d)		67.6	52.7
CASSCF(12,10)/6-31G(d,p)// B3LYP/6-31G(d)	96.8		
CASSCF(18,14)/6-31G(d,p)// B3LYP/6-31G(d)		61.4	53.6
Open-Shell Singlet at Relaxed Geometry ^b			
CASSCF(4,3)/6-31G(d,p)	d		
CASSCF(6,4)/6-31G(d,p)		27.0	21.1
CASSCF(6,5)/6-31G(d,p)	42.6		
CASSCF(8,6)/6-31G(d,p)		30.2	20.5
CASSCF(12,10)/6-31G(d,p)	54.9		
Triplet ^c			
CBS-QB3	24.4	-15.7	-13.8
B3LYP/6-31G(d)	15.2	-23.0	-20.5
B3LYP/6-311+G(d,p)// B3LYP/6-31G(d)	15.1	-22.9	-22.2
CASSCF(4,3)/6-31G(d,p)	4.4		
CASSCF(6,4)/6-31G(d,p)		-31.4	-27.1
CASSCF(6,5)/6-31G(d,p)	7.3		
CASSCF(8,6)/6-31G(d,p)		-31.6	-22.7
CASSCF(12,10)/6-31G(d,p)	28.7		
CASSCF(4,3)/6-31G(d,p)// B3LYP/6-31G(d)	3.3		
CASSCF(6,4)/6-31G(d,p)// B3LYP/6-31G(d)		-34.4	-27.8
CASSCF(6,5)/6-31G(d,p)// B3LYP/6-31G(d)	9.4		
CASSCF(8,6)/6-31G(d,p)// B3LYP/6-31G(d)		-31.5	-27.5
CASSCF(12,10)/6-31G(d,p)// B3LYP/6-31G(d)	29.5		
CASSCF(18,14)/6-31G(d,p)// B3LYP/6-31G(d)		-30.7	-22.8

^a Energy difference reported in kilocalories per mole. The CASSCF and B3LYP/6-31G(d) values are bottom-of-the-well energy differences. The CBS-QB3 and B3LYP/6-311+G(d,p)//B3LYP/6-31G(d) energy differences represent ΔG at 298 K. A positive value indicates that the closed-shell singlet state is lower in energy for that nitrene at that level of theory. ^b Energy difference between closed-shell singlet state and open-shell singlet state. ^c Energy difference between the closed-shell singlet state and the open-shell triplet state. ^d SCF did not converge.

Curtius-like Rearrangement. For phosphinoyl, phosphinyl, and phosphoryl azides, the products isolated from the thermal and photochemical reactions indicate that there can be two important reaction pathways. Both of these reaction pathways involve the loss of nitrogen. In one case, the loss of nitrogen is in concert with a Curtius-like rearrangement, and the other pathway leads to simple formation of the nitrene. In principle, the Curtius-like rearrangement could occur from the nitrene after the loss of molecular nitrogen. We refer to the Curtius-like rearrangement directly from the azide as the concerted pathway, and the pathway in which the azide forms the nitrene that then

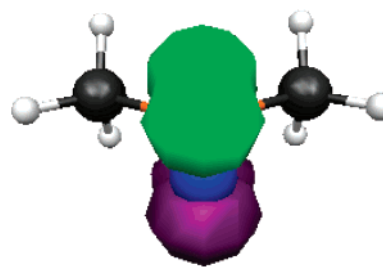
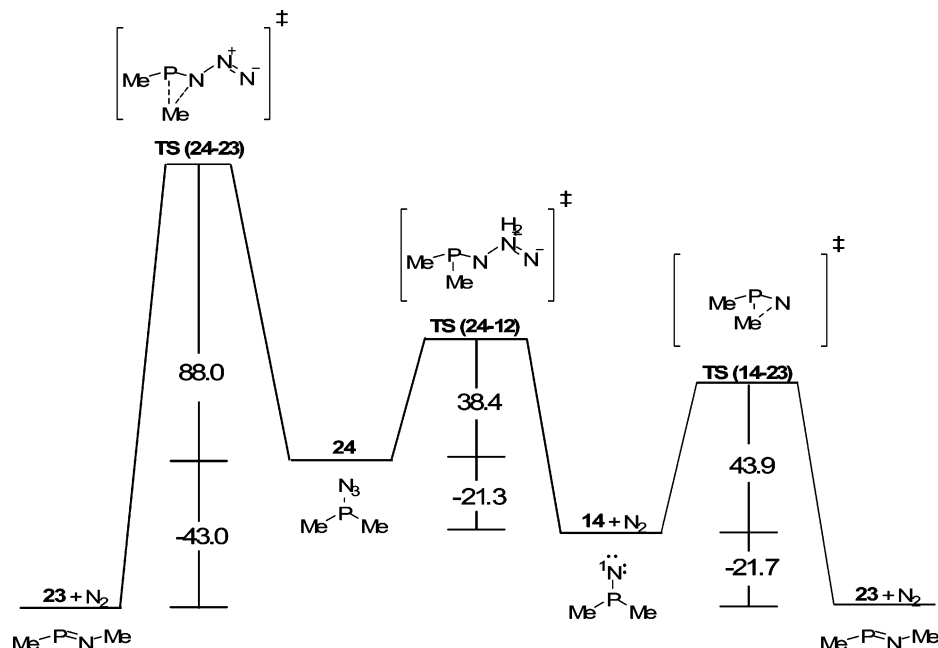


FIGURE 5. Highest occupied (natural) molecular orbital of dimethylphosphinoylnitrene at the CASSCF(6,5)/6-31G(d,p) level of theory, rendered with a contour value of 0.295 au and illustrating the phosphorus–nitrogen π bond.

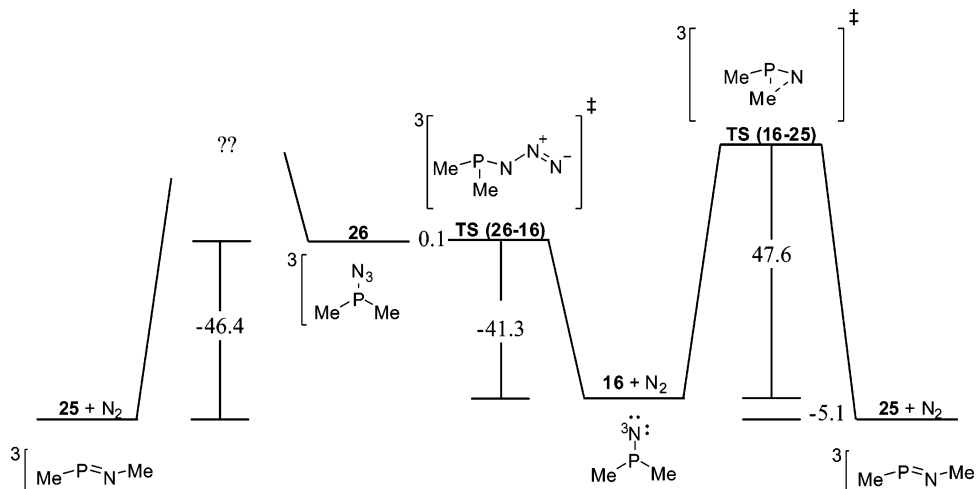
undergoes Curtius-like rearrangement is discussed as the stepwise pathway. To determine if the thermal Curtius-like rearrangement occurs from the azide precursor or the subsequent nitrene, the concerted and stepwise Curtius-like rearrangements of dimethylphosphinoyl, dimethylphosphinyl, and dimethylphosphoryl azide for both the closed-shell singlet and the triplet states have been examined using B3LYP and CBS-QB3 methods. The results of these calculations are shown in Schemes 1–6. In the schemes, the pathway leading backward (left) from the azide represents the concerted Curtius-like rearrangement, and the pathway moving forward (right) from the azide represents the stepwise pathway. The energy differences between the stationary points (the azides, products, intermediates, and transition states) along the pathways are CBS-QB3 free energies at 298.15 K, and unless stated otherwise, these are the values discussed in the text. The CBS-QB3 values are considered to be the most reliable because they constitute a CCSD(T) calculation along with a complete basis set extrapolation. Complete tables containing the free energies of reaction and the activation barriers at the B3LYP/6-311+G(d,p)//B3LYP/6-31G(d) level of theory can be found in the Supporting Information. Typically, the B3LYP/6-311+G(d,p)//B3LYP/6-31G(d) values were within 5 kcal mol⁻¹ of the CBS-QB3 results.

Dimethylphosphanoyl Azide. The Curtius-like rearrangement for dialkylphosphinoyl azides has not been observed thermally or photochemically.²⁶ The two important reaction pathways of dimethylphosphinoyl azide in the closed-shell singlet and the triplet state are shown in Schemes 1 and 2, respectively. The transition state for the concerted Curtius-like rearrangement (**TS (24–23)**) was found at the B3LYP/6-31G(d) level of theory. However, when this geometry was used as a starting geometry for the geometry optimization of the CBS-QB3 procedure, a concerted Curtius-like transition state could not be obtained. In an attempt to locate the CBS-QB3 transition-state geometry, the optimization step size and starting geometries were varied, but these efforts were unsuccessful. The free energy of activation (ΔG^\ddagger) for **TS (24–23)** at the B3LYP/6-311+G(d,p)//B3LYP/6-31G(d) level of theory was found to be 88.0 kcal mol⁻¹, which is the value given in Scheme 1. All other values in Scheme 1 are CBS-QB3 free energies. Attempts to find a triplet, concerted, Curtius-like rearrangement transition state were unsuccessful. Reasonable starting geometries for the transition-state searches were constructed from nitrene transition states by changing the nitrenes into azides without any perturbation of the transition-state structure. These constructed geometries were then optimized while constraining

(26) Majoral, J. P.; Bertrand, G.; Ocando-Marquez, E.; Baceiredo, A. *Bull. Soc. Chim. Belg.* **1986**, *95*, 945.

SCHEME 1. Reaction Pathways for Concerted and Stepwise Rearrangement of Dimethylphosphinoyl Azide via the Closed-Shell Singlet State^a


^a Energies are listed as free energies (298 K, kcal mol⁻¹) at the CBS-QB3 level of theory, except for TS (24–23). The ΔG^\ddagger TS (24–23) value was obtained at the B3LYP/6-311+G(d,p)/B3LYP/6-31G(d) level of theory.

SCHEME 2. Reaction Pathways for Concerted and Stepwise Rearrangement of the Triplet Dimethylphosphinoyl Azide and Triplet State of the Nitrene^a


^a Energies are listed as free energies (298 K, kcal mol⁻¹) at the CBS-QB3 level of theory.

key internal coordinates or performing relaxed scans along the N–N₂ bond. From these optimizations and relaxed scans, new starting geometries were used in saddle point searches that resulted in transition states where either the nitrogen had predissociated or that led directly to the nitrene. The free energy of reaction (ΔG) of the rearrangement was exoergic by -43.0 and -46.4 kcal mol⁻¹ for the singlet and triplet states, respectively.

In the triplet state, the loss of nitrogen proceeds with virtually no barrier to the nitrene that is exoergic by -41.3 kcal mol⁻¹. The ΔG^\ddagger for the loss of nitrogen leading to the formation of the closed-shell singlet nitrene is $+38.4$ kcal mol⁻¹, and the reaction is exoergic by -21.3 kcal mol⁻¹. The ΔG^\ddagger for the concerted pathway is much higher (88.0 kcal mol⁻¹) than loss

of nitrogen leading to the formation of the nitrene. Therefore, it is expected that the pyrolysis of dimethylphosphinoyl azide will lead exclusively to the nitrene intermediate. However, there is no experimental evidence to compare with the calculated data in this report.

For dimethylphosphinoylnitrene, the ΔG for the Curtius-like rearrangement is -21.7 kcal mol⁻¹ for the closed-shell singlet state and -5.1 kcal mol⁻¹ for the triplet state. The ΔG^\ddagger values are $+43.9$ and $+47.6$ kcal mol⁻¹ for the closed-shell singlet and triplet nitrene, respectively. The closed-shell singlet and triplet state B3LYP/6-31G(d) transition-state geometries of dimethylphosphinoylnitrene are shown in Figure 4. In addition to the geometries of the transition states, the values of key bond lengths and angles for the nitrene (starting material, (SM),

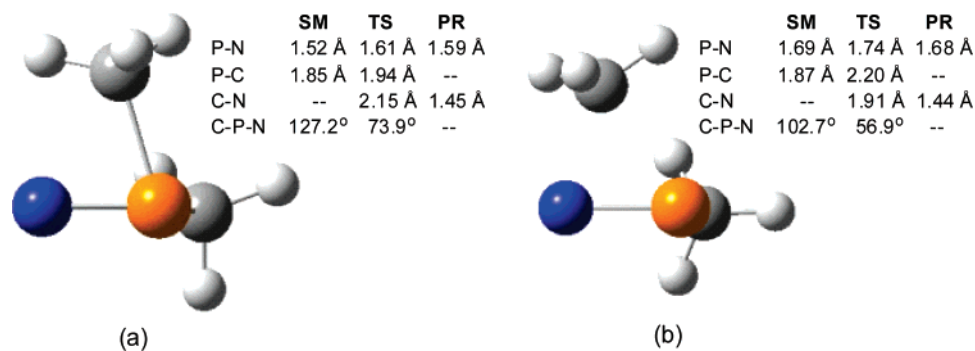
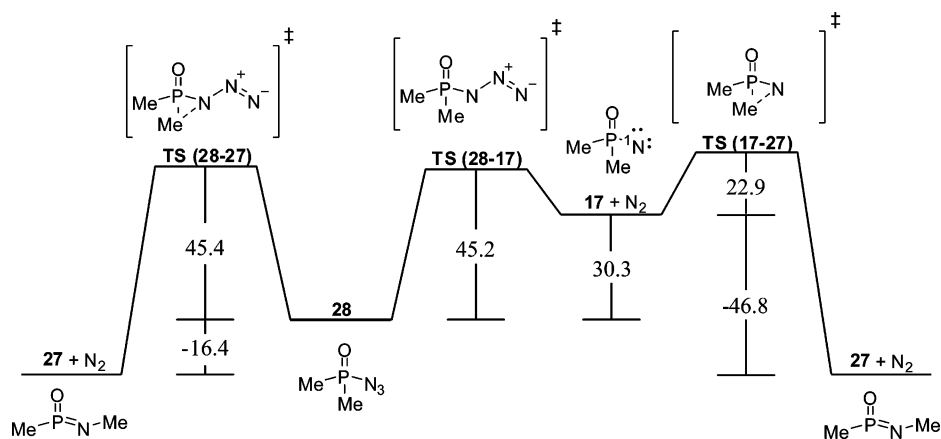


FIGURE 6. Phosphinoylnitrene Curtius-like rearrangement transition states. (a) Singlet nitrene B3LYP/6-31G(d) Curtius-like rearrangement transition state. (b) Triplet nitrene B3LYP/6-31G(d) Curtius-like rearrangement transition state.

SCHEME 3. Reaction Pathways for Concerted and Stepwise Rearrangement of Dimethylphosphinyl Azide via the Closed-Shell Singlet State^a



^a Energies are listed as free energies (298 K, kcal mol⁻¹) at the CBS-QB3 level of theory.

transition states (TS), and *E*-methyl(methylimino)phosphine product (PR)) are given in Figure 6. The closed-shell singlet nitrene Curtius-like rearrangement is 16.6 kcal mol⁻¹ more exoergic than the triplet state and should have an earlier transition state. The P–C bond of the closed-shell singlet transition state has lengthened only by 0.09 Å compared to the triplet state where the bond has lengthened 0.33 Å in the transition state, which is consistent with the closed-shell singlet having an earlier transition state. Bimolecular reactions limit the lifetimes of most nitrene to be submicrosecond. The Curtius-like rearrangement barriers for the closed-shell singlet and triplet states of dimethylphosphinoylnitrene are both more than 40 kcal mol⁻¹. Because of these large barriers, the reaction will essentially not occur at room temperature. If dimethylphosphinoylnitrene forms as an intermediate, a bimolecular reaction will occur, thereby prohibiting the Curtius-like rearrangement. Therefore, the predicted thermal reaction pathway of dimethylphosphinoyl azide is to extrude nitrogen to form the closed-shell singlet phosphinoylnitrene, which will then react in a bimolecular fashion without undergoing a Curtius-like rearrangement.

Dimethylphosphinyl Azide. The photochemical reactions of diaryl- and dialkylphosphinyl azides have been well studied, and in all cases, the Curtius-like rearrangement products were the major products.^{6–8} Thermally, no experimental investigation has been reported. The thermal concerted and stepwise reaction pathways leading to the *Z*-methylphosphonimidate (27) from dimethylphosphinyl azide (28) for the closed-shell singlet state

and triplet state are shown in Schemes 3 and 4, respectively. Again, the transition state for the triplet state concerted Curtius-like rearrangement could not be located for reasons similar to those experienced in the case of dimethylphosphinoyl azide. The ΔG for the concerted Curtius-like rearrangement is exoergic for both the singlet (–16.4 kcal mol⁻¹) and triplet states (–44.1 kcal mol⁻¹). Despite being exoergic, the ΔG^\ddagger for the thermal Curtius-like rearrangement of the singlet phosphinyl azide is a substantial +45.4 kcal mol⁻¹. Interestingly, the corresponding barrier for the extrusion of nitrogen to form the closed-shell singlet nitrene is +45.2 kcal mol⁻¹, which is very similar to the rearrangement barrier. Thus, we predict that the thermolysis of dimethylphosphinyl azide should lead to a competition between the formation of the nitrene and rearrangement product. In the triplet state, loss of nitrogen is exoergic by –44.1 kcal mol⁻¹ and is essentially barrierless.

The rearrangement of the closed-shell singlet dimethylphosphinoylnitrene (17) to 27 is highly exoergic. The free energy of reaction is –46.8 kcal mol⁻¹, and the activation barrier is +22.9 kcal mol⁻¹. The Curtius-like rearrangement of triplet phosphinoylnitrene has a substantial activation barrier of +53.7 kcal mol⁻¹, and the free energy of reaction is 0.0 kcal mol⁻¹. Once dimethylphosphinoylnitrene has been formed by photolysis or pyrolysis, the +22.9 and +53.7 kcal mol⁻¹ ΔG^\ddagger barriers prohibit the Curtius-like rearrangement in both the closed-shell singlet and triplet states of the nitrene, respectively. The +22.9 kcal mol⁻¹ barrier for the closed-shell singlet phosphinoylnitrene

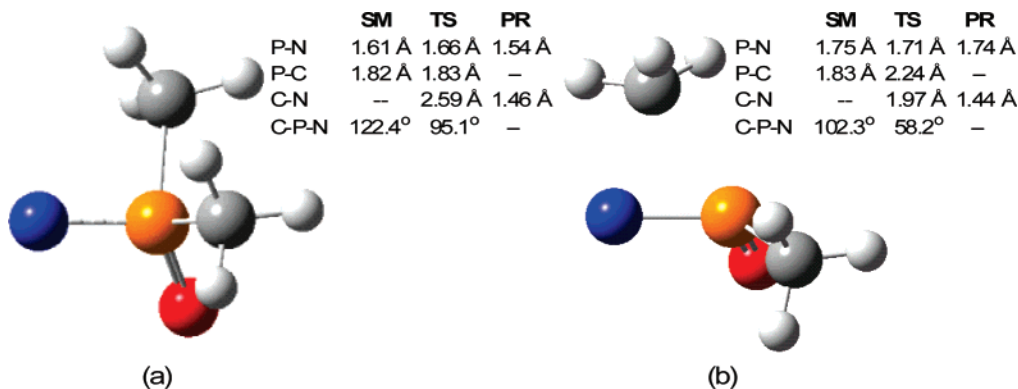
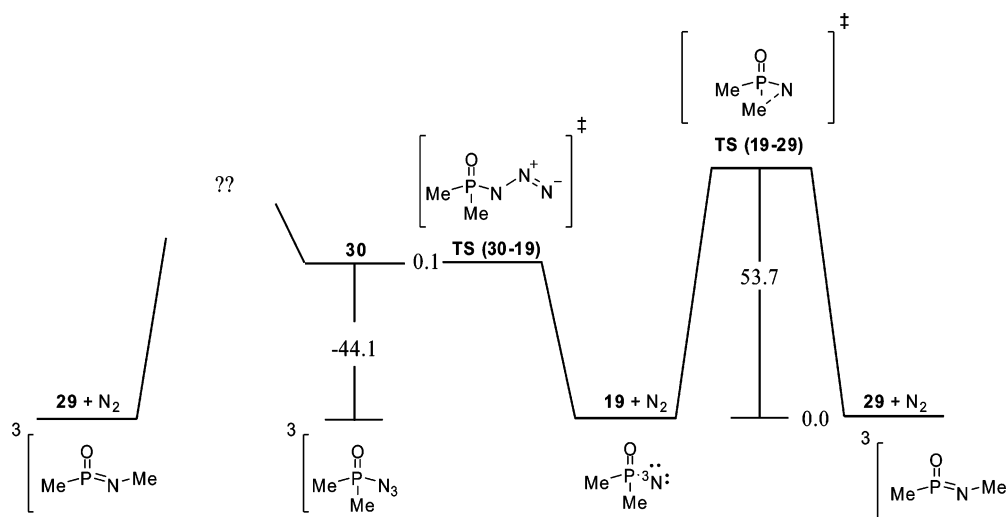


FIGURE 7. Phosphinoylnitrene Curtius-like rearrangement transition states. (a) Singlet nitrene B3LYP/6-31G(d) Curtius-like rearrangement transition state. (b) Triplet nitrene B3LYP/6-31G(d) Curtius-like rearrangement transition state.

SCHEME 4. Reaction Pathways for Concerted and Stepwise Rearrangement of the Triplet Dimethylphosphinyl Azide and Triplet State of the Nitrene^a



^a Energies are listed as free energies (298 K, kcal mol⁻¹) at the CBS-QB3 level of theory.

Curtius-like rearrangement is much too high to allow competition with typical bimolecular nitrene chemistry.

The transition states for the closed-shell singlet and triplet phosphinoylnitrene Curtius-like rearrangements are shown in Figure 7. As in the case of dimethylphosphinoylnitrene, the closed-shell singlet nitrene has a substantially more exoergic Curtius-like rearrangement than the triplet nitrene. The exoergic nature of the Curtius-like rearrangement for the closed-shell singlet state manifests itself in the transition state being earlier than for the triplet state, as was observed for phosphinoylnitrene. The bonds being broken and formed are the ones most affected by the earliness or lateness of the transition state. For the closed-shell singlet nitrene, the P–C bond has barely changed (0.01 Å) and the C–P–N bond angle has decreased by 27.3° in the transition state. The P–C bond has lengthened significantly (0.41 Å), and the C–P–N bond angle has decreased by 44.1° in the triplet nitrene transition state. The large difference in the progress of the P–N bond lengthening (breaking) is evidence for the early nature of the closed-shell singlet nitrene's transition state.

Dimethylphosphoryl Azide. The concerted and stepwise pathways for the closed-shell singlet state of dimethylphosphoryl azide are shown in Scheme 5. Unlike the rearrangement of dimethylphosphinyl azide (**30**) to **29**, which was exoergic (–16.4

kcal mol⁻¹), the rearrangement of dimethylphosphoryl azide (**32**) to *Z*-dimethylphosphonamidate (**31**) in the singlet state is endothermic by 28.7 kcal mol⁻¹. The increase in endothermicity is reflected in a slightly larger activation barrier of +47.0 kcal mol⁻¹ for the Curtius-like rearrangement of **32**, which is slightly larger than that of **30** (+45.4 kcal mol⁻¹). Qualitatively, the endothermicity of the Curtius-like rearrangement of **32**, as compared to exoergic rearrangement of **30**, can be rationalized by considering the relative bond strengths of the products. The experimental bond dissociation energies of a O₂N–OCH₃ and a O₂N–CH₃ bond can be estimated to be approximately 42.0 and 61.0 kcal mol⁻¹, respectively.²⁷ The Curtius-like rearrangement of **30** to **29** is stabilized by the greater bond strength of the N–C bond compared to the N–O bond formation arising from the Curtius-like rearrangement of **32**.

The observed products of the photolysis of diphenoxyphosphoryl azide contained no phosphonamidate arising from a Curtius-like rearrangement and were exclusively C–H insertion products derived from the nitrene.⁴ There are also no known experimental examples of a phosphoryl azide yielding Curtius-like rearrangement products. The Δ*G*[‡] for the release of nitrogen

(27) Blanksby, S. J.; Ellison, G. B. *Acc. Chem. Res.* **2003**, *36*, 255–263.

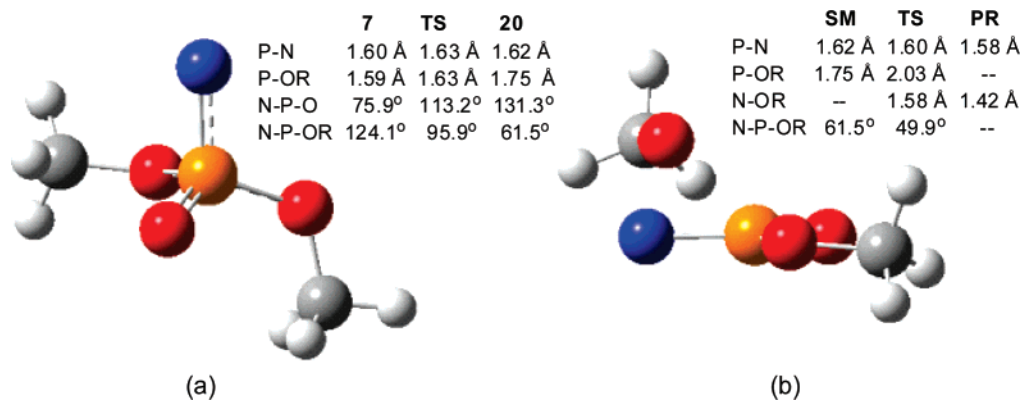
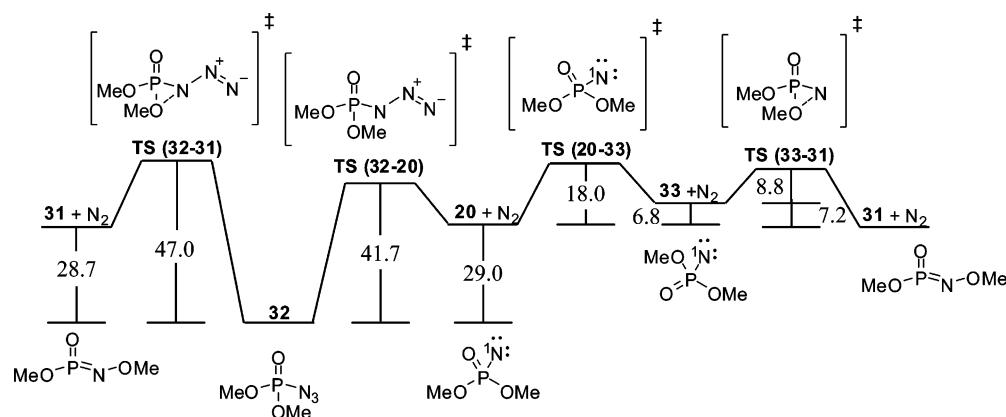


FIGURE 8. Closed-shell singlet phosphorylnitrene Curtius-like rearrangement transition states. (a) Singlet nitrene B3LYP/6-31G(d) transition state leading from **20** to **33**. (b) B3LYP/6-31G(d) Curtius-like rearrangement transition state from **33** leading to the product.

SCHEME 5. Reaction Pathways for Concerted and Stepwise Rearrangement of Dimethylphosphoryl Azide via the Closed-Shell Singlet State^a



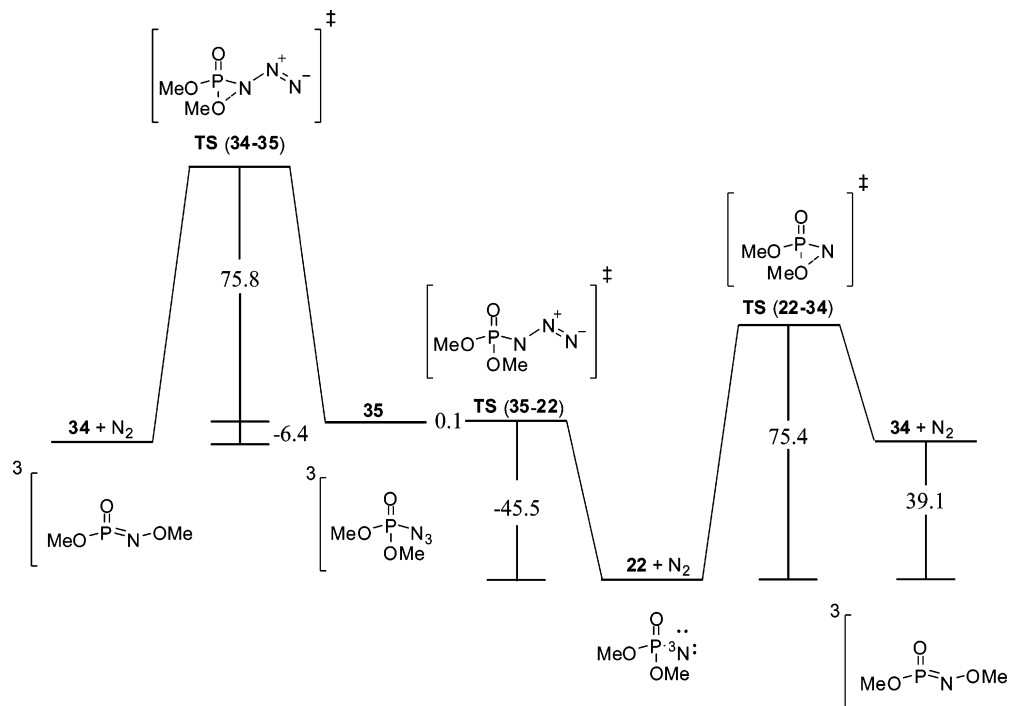
^a Energies are listed as free energies (298 K, kcal mol⁻¹) at the CBS-QB3 level of theory.

to form the singlet nitrene was +41.7 kcal mol⁻¹, which is 5.3 kcal mol⁻¹ lower in energy than the Curtius-like rearrangement barrier. The lower barrier for the extrusion of nitrogen will favor the formation of phosphorylnitrene over rearrangement to the phosphoramidate during pyrolysis. Thus, the predicted thermal reactions of phosphoryl azides yield products similar to those arising from photolysis because of chemistry from the incipiently formed nitrene.

Change from methyl to methoxy substituents affects the stepwise (nitrene) Curtius-like rearrangement reaction pathway for the closed-shell singlet state. In addition to the phosphoryl oxygen, the weak N^{•••}O interaction, previously observed in acylnitrenes²¹ and now for phosphorylnitrenes, can also form between the methoxy oxygen and nitrogen. When this weak interaction involves the phosphoryl oxygen (**20**) instead of one of the methoxy substituents (**33**), the closed-shell singlet phosphorylnitrene is stabilized by 6.8 kcal mol⁻¹. However, it is necessary for the nitrogen of the phosphorylnitrene to first associate with the methoxy substituent undergoing the 1,2-migration before the Curtius-like rearrangement can take place. Following the intrinsic reaction coordinate backward from the transition state leading to the product (**31**) led to structure **33**. No transition state connecting **20** and **31** could be found. The transition state leading from **20** → **33** (TS **20–33**), shown in Figure 8a, has a skewed tetrahedral geometry with the normal coordinate for the imaginary vibrational frequency corresponding to the nitrogen in metronomic motion between the phosphoryl

oxygen and a methoxy substituent. In TS (**20–33**), the N–P–O bond angle increases by 37.3° and the N–P–OMe bond angle decreases by 28.2° from the closed-shell singlet minimum **7**, and these changes are 67% and 45% toward their eventual values in **33**, respectively. However, the P–OMe bond length has only increased 0.04 Å in the transition state or 25% toward its value in **33**. Figure 8b shows the transition-state geometry leading from **33** to **31**. The P–OMe bond increase of 0.18 Å in the transition state is well advanced compared to the closed-shell singlet phosphorylnitrene whose P–C bond has only lengthened by 0.01 Å.

The activation barriers from **20** → **33** and **33** → **31** were +18.0 and +8.8 kcal mol⁻¹, respectively. Therefore, the rate-limiting step involves breaking the weak interaction between nitrogen and the phosphoryl oxygen, followed by the formation of an interaction between the nitrogen and the methoxy oxygen. For dimethylphosphorylnitrene (**17**), the breaking of the weak interaction between nitrogen and the phosphoryl oxygen occurs in the same step as the 1,2-methyl shift. The ability of the closed-shell singlet of **20** to regain this interaction with the methoxy group in structure **33** allows the 1,2-methoxy migration to occur with a lower free energy of activation barrier through a two-step Curtius-like rearrangement. Even though the Curtius-like rearrangement takes place in two steps, the ΔG[‡] of +18.0 kcal mol⁻¹ in the rate-limiting step for the Curtius-like rearrangement of closed-shell singlet phosphorylnitrene is prohibitive. Again, the size of this barrier does not allow the Curtius-like rear-

SCHEME 6. Reaction Pathways for Concerted and Stepwise Rearrangement of the Triplet Dimethylphosphoryl Azide and Triplet State of the Nitrene^a

^a Energies are listed as free energies (298 K, kcal mol⁻¹) at the CBS-QB3 level of theory.

rearrangement to compete with the normal bimolecular reactions of the nitrene.

Unlike the dimethylphosphinoyl and dimethylphosphinyl azides, the transition state leading from triplet dimethylphosphoryl azide (**35**) was located. The ΔG and ΔG^\ddagger for the concerted Curtius-like rearrangement of triplet phosphoryl azide are -6.4 and $+75.8$ kcal mol⁻¹, respectively. As before with the other triplet azides, **35** extrudes nitrogen with virtually no barrier to form the corresponding triplet nitrene, which is exoergic by -45.5 kcal mol⁻¹. The Curtius-like rearrangement of triplet dimethylphosphorylnitrene must overcome a large free energy of activation of $+75.4$ kcal mol⁻¹. The size of the activation barrier is reflective of the triplet Curtius-like rearrangement being endoergic by $+39.1$ kcal mol⁻¹. The concerted and stepwise reaction pathways of triplet dimethylphosphoryl azide are shown in Scheme 6.

For all of the examined nitrenes, the Curtius-like rearrangements must surmount substantial activation barriers, and thus, it is likely that the Curtius-like rearrangements of all of the examined nitrenes will be prohibited. To further support this conclusion, it can be noted that the Curtius-like rearrangement activation barrier of $+18.0$ kcal mol⁻¹ for the rate-limiting step of the closed-shell singlet dimethylphosphorylnitrene (**20**) is lower than the activation barrier for dimethylphosphinyl nitrene (**17**). The lower activation barrier of the closed-shell singlet **20** would suggest that the Curtius-like rearrangement would be even more favorable for phosphorylnitrenes (**20**) than that for phosphinyl nitrenes (**17**). Yet, Curtius-like rearrangements have not been observed for phosphoryl azides or their corresponding nitrenes.⁴ Thus, if the more energetically favorable Curtius-like rearrangement does not occur for phosphorylnitrenes, it is unlikely that phosphinyl nitrenes will undergo the Curtius-like rearrangement.

However, it is known that phosphinyl azides upon photolysis will undergo a Curtius-like rearrangement.⁶⁻⁸ Assuming the

prediction made in this report that there are no feasible thermal Curtius-like rearrangement pathways for the azide is correct, there are a few other possible explanations for this observation. First, the Curtius-like rearrangement could occur from the excited state of the phosphinyl azide. The other explanation is that the Curtius-like rearrangement occurs from a vibrationally "hot" state of the nitrene before it can relax. In either case, this is consistent with the previous assertion that the Curtius-like rearrangement of phosphinyl azides occurs in a concerted manner without the formation of a phosphinyl nitrene intermediate.⁸

We can only speculate on why Curtius-like rearrangement is only photochemically observed for phosphinyl azide, and not phosphinoyl or phosphoryl azide. One relevant observation can be made from the free energies of reaction for the corresponding nitrenes. The rearrangement products of phosphinyl azide are -46.8 kcal mol⁻¹ exoergic compared to the closed-shell singlet nitrene. This is substantially more exoergic than phosphinoyl- and phosphorylnitrenes whose Curtius-like rearrangement products are only -21.7 and -0.3 kcal mol⁻¹ exoergic, respectively, compared to their corresponding nitrenes. The favorable energetics of the Curtius-like rearrangement for phosphinyl azide compared to the formation of phosphinyl nitrene may lead to a decrease in the barrier to rearrangement on the excited singlet state surface to a point where it begins to compete with the formation of nitrene. For phosphinoyl and phosphoryl azide, the activation barrier to rearrangement on the excited state surface may be intrinsically higher because of the less favorable energetics.

Conclusions

A number of chemical insights into the chemistry of phosphinoyl, phosphinyl, and phosphoryl azides have been made in this report. One such insight is the nature of the electronic states

of the examined nitrenes. Calculations performed at the CASSCF level of theory show that the closed-shell singlet states of dimethylphosphinoyl-, dimethylphosphinyl- and dimethylphosphorylnitrenes are lower in energy than the open-shell singlet configuration. In the closed-shell singlet state of dimethylphosphinyl- and dimethylphosphorylnitrene, a weak interaction between a lone pair orbital on the phosphoryl oxygen and an empty p orbital on nitrogen resulted in a structure similar to those that have been observed for acylnitrenes.²⁴ However, unlike acylnitrenes, which have a closed-shell singlet ground state, the triplet states of phosphinyl- and phosphorylnitrene are the ground states. Thus, the stabilization of the closed-shell singlet by the weak $N\cdots O$ is sufficient to make the closed-shell singlet the lowest energy singlet but not the ground state. Unlike phosphinyl- and phosphorylnitrenes, phosphinoylnitrene closed-shell singlet is the ground state. The closed-shell singlet of phosphinoylnitrene is stabilized by a π bond between the phosphorus and nitrogen atoms. The formation of this π bond is prevented in phosphinyl and phosphoryl singlet nitrene by the P–O bond, which contains the p orbital on the phosphorus atom that contributes to the π bond. The accuracy of the CASSCF calculations was calibrated by the CBS-QB3 singlet–triplet energy gaps. The inclusion of dynamic electron energies correlation and the largest practical active space is desirable for accurate calculation of the singlet–triplet energy gaps, but qualitative values can be obtained as long as the important valence orbitals associated with the nitrogen of the nitrene are included in the active space.

The results provided in this report also give a detailed energetic description of the possible Curtius-like rearrangement pathways of the examined azides. During the pyrolysis of dimethylphosphinoyl azide, the lower ΔG^\ddagger (38.4 kcal mol⁻¹) should heavily favor the loss of nitrogen to form an intermediate nitrene over a Curtius-like rearrangement ($\Delta G^\ddagger = 88.0$ kcal mol⁻¹). Once dimethylphosphinoylnitrene is formed, the Curtius-like rearrangement would be prevented by a substantial barrier (43.9 kcal mol⁻¹) and bimolecular nitrene chemistry is expected. For dimethylphosphinyl azide, a concerted Curtius-like rearrangement has an activation barrier that is essentially the same as the barrier for the formation of the phosphinoylnitrene. Thus, the thermolysis of phosphinyl azide should lead to a mixture of Curtius-like rearrangement and nitrene products. The phos-

phinylnitrene intermediate is not expected to undergo a Curtius-like rearrangement because of an activation barrier (22.9 kcal mol⁻¹) that renders the Curtius-like rearrangement noncompetitive with much faster bimolecular reactions. For dimethylphosphoryl azide, the barrier to the formation to nitrene is 5.3 kcal mol⁻¹ less than the activation barrier for Curtius-like rearrangement, and the majority of observed products from pyrolysis should arise from the nitrene. The Curtius-like rearrangement of the closed-shell singlet of phosphorylnitrene proceeds in two steps where the first step is the formation of a structure where a methoxy substituent has associated with the nitrogen of the phosphorylnitrene. From this intermediate, the Curtius-like rearrangement takes place. The separation of the phosphorylnitrene Curtius-like rearrangement into two steps results in a rate-limiting activation barrier (18.0 kcal mol⁻¹) that is lower than the activation barrier for the one-step phosphinoylnitrene (22.9 kcal mol⁻¹) Curtius-like rearrangement. Even though the Curtius-like rearrangement from the closed-shell singlet phosphorylnitrene has the lowest free energy of activation, rearrangement products have not been observed experimentally. Therefore, it is unlikely that the Curtius-like rearrangement will effectively compete with bimolecular reactions for any of the examined nitrenes.

Last, the extrusion of nitrogen to form the triplet nitrene proceeds with virtually no barrier in all cases. Thus, the formation of any of the examined triplet azides will lead exclusively to the corresponding triplet nitrene. The CBS-QB3 calculated free-energy activation barriers for the Curtius-like rearrangement of triplet phosphinoyl-, phosphinyl-, and phosphorylnitrene are +47.6, +53.7, and +75.4 kcal mol⁻¹, respectively. These barriers prohibit the Curtius-like rearrangement, and only triplet nitrene derived products should be observed.

Acknowledgment. Financial and computational support of this work by the NIH, NSF, and Ohio Supercomputer Center is gratefully acknowledged.

Supporting Information Available: Tables of energies, Cartesian coordinates, vibrational frequencies, and selected figures of computational results. This material is available free of charge via the Internet at <http://pubs.acs.org>.

JO0711687